

MINERALOGY AND ^{15}N -RICH ORGANIC MATTER IN THE FINE-GRAINED ANTARCTIC MICROMETEORITE T98G8: EVIDENCE FOR A COMETARY ORIGIN? P. Haenecour¹, J. Y. Howe^{1,2}, T. J. Zega^{1,3}, P. Wallace¹, M. Atsushi², S. Takeshi⁴, K. Kaji⁴, C. Floss⁵, T. Yada⁶. ¹Lunar and Planetary Laboratory, The University of Arizona, Tucson, AZ, USA. ²Hitachi High-Technologies America Inc., Clarksburg, USA. ³Dept. of Materials Science and Engineering The University of Arizona, Tucson, AZ, USA. ⁴Hitachi High-Technologies Corporation, Hitachinaka, Japan. ⁵Physics Dept. and Laboratory for Space Sciences, Washington University, St. Louis, MO, USA. ⁶JAXA, Institute of Space and Astronautical Science, Kanagawa, Japan. (pierre@lpl.arizona.edu).

Introduction: Antarctic micrometeorites (AMMs) are small ($\sim 50\ \mu\text{m}$ to 1 mm) extraterrestrial particles typically collected from melting Antarctic snow or blue ice [1]. They are of particular interest, because they may have contributed a significant amount of water and organics to the early Earth [2]. However, their origin(s) and possible relationships to other extraterrestrial materials are still debated, and both asteroidal (related to chondrites) and cometary (related to interplanetary dust particles, IDPs) origins have been proposed [2-4].

Deuterium- and ^{15}N -rich organic matter has been reported in AMMs [3, 4]. Similarly to carbonaceous chondrites, a recent study of N-rich organic matter in an ultracarbonaceous AMMs indicated the presence of similar functional groups (e.g., aromatic carbon, nitrile, carboxyl) [5]. However, very few studies have investigated the diversity of isotopic compositions and functional chemistry of organic matter in fine-grained AMMs. Here, we report new data on the isotopic and elemental compositions and functional chemistry of ^{15}N -rich hotspots in a fine-grained micrometeorite.

Experimental Methods: Using the Cameca NanoSIMS 50 at Washington University in St Louis, we carried out raster ion imaging of C and N isotopes in multi-collection mode in three fine-grained AMMs (T98G8, T00Iba030 and T98G5) to identify isotopic anomalies. A focused Cs^+ primary beam of $\sim 1\ \text{pA}$ ($\sim 100\ \text{nm}$) was rastered over surface areas of $15 \times 15\ \mu\text{m}^2$. We mapped a total area of $26,500\ \mu\text{m}^2$. The N and C isotopic compositions were normalized to synthetic Si_3N_4 and SiC standards, respectively. Electron-transparent cross-sections of three ^{15}N -rich hotspots (T98G8-E4, T98G8-C13-1 and T98G8-C13-2) identified in T98G8 were then prepared for additional study in the new Hitachi SU9000 30kV SEM/STEM with Oxford Instruments X-Max 100LE EDS detector, and the 60-200 keV Hitachi HF5000 TEM/STEM at the University of Arizona (UA). The cross-sections were prepared using the dual-beam Thermo Scientific Helios NanoLab 660 FIB scanning electron microscope at UA, via previously described focused-ion-beam techniques [6]. We acquired high-resolution images, EDS elemental maps and energy electron-loss spectroscopy (EELS) measurements of these hotspots.

Results and Discussion: Recently, nitrogen isotopic anomalies and high presolar grain abundances were identified in a primitive AMM, T98G8 [7]. High presolar grain abundances, like those seen in the most primitive carbonaceous chondrites, were also identified in several other fine-grained AMMs [1, 8]. We found new additional ^{15}N -rich hotspots in the AMMs T9898 and T00Iba030. Unlike the matrix in many CR chondrites, T98G8 and T00Iba030 have bulk $^{14}\text{N}/^{15}\text{N}$ ratio close to normal values ($^{14}\text{N}/^{15}\text{N} = 261$ and 282, respectively; Fig. 1). We identified several ^{15}N -rich hotspots in both AMMs, and the three hotspots in T98G8 that we extracted for TEM studies are all characterized by moderate enrichments in ^{15}N ($\delta^{15}\text{N} \approx 200\%$).

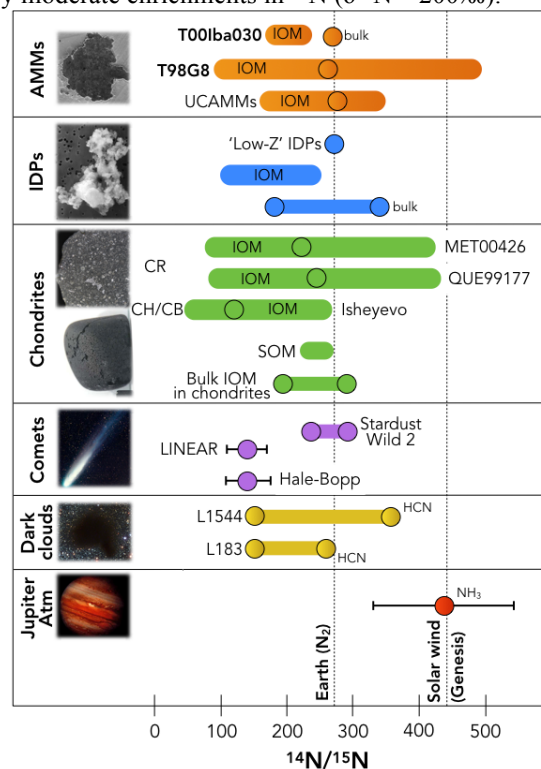


Fig. 1: Nitrogen isotopic compositions ($^{14}\text{N}/^{15}\text{N}$) of Solar System objects compared to AMMs. Black lined circles correspond to bulk nitrogen isotopic compositions ('bulk') and colored areas correspond to ranges of N-anomalous hotspots ('IOM' = insoluble organic matter; 'SOM' = soluble organic matter). Data for T98G8 and T00Iba030 are from this study. Other data are from [9-12 and references therein].

The bright-field images and EDS elemental maps show that the AMM T98G8 is composed mostly of silicate grains mixed in a fine-grained groundmass of oxide, silicate and C-rich grains, without any sign of aqueous alteration (e.g., hydrous minerals; Fig. 2). The high presolar silicate abundances is also consistent with minimal secondary processing [1, 8]. In addition to the ^{15}N -rich hotspots, the EDS maps show the presence of carbonaceous matter throughout the AMM.

While being characterized by similar ^{15}N enrichments, the three hotspots show different structures and compositions. T98G8-C13-2 is composed of a hollow nanoglobule and is surrounded by GEMS-like material (glass with embedded metal and sulfides) typically identified in interplanetary dust particles (IDPs; Fig. 3). In comparison, T98G8-C13-1 is larger (1.8 μm long) and more complex with silicate and oxide grains mixed together in diffuse carbonaceous material (Fig. 2). Hotspot T98G8-E4 is characterized by a C-rich globule-like grain with a silicate inclusion in the center. Adjacent to this latter hotspot is also a small broken and globule-like grain filled with silicate and oxide grains (Fig. 2). Our observations in T98G8 are similar to previous studies of primitive chondritic porous (CP) IDPs [13], suggesting that T98G8 might be composed of CP-IDP-like material and might, thus, also have a cometary origin. While its presolar silicate abundance (191 ± 38 ppm) is lower than those observed in IDPs [14], discrete areas in T98G8 are characterized by much higher abundances (~ 650 ppm; [1]).

Our initial EELS data on several C-rich regions in hotspot T98G8-E4 suggests that they are mainly composed of aromatic carbon, with a energy-loss near-edge structure (ELNES) for C, K edge containing a sharp rise from edge onset to a peak at 285 eV (the π^* peak) and a delayed maximum at ~ 290 eV (the σ^* peak). We did not identify any other significant edges (e.g., S, N, or O) in the EELS spectra. Prior to the meeting, we will compare these results with several additional hotspots in T001ba030, and carry out detailed electron diffraction and EELS measurements using the Hitachi HF5000.

References. [1] Yada et al. (2008) MAPS 43, 1287. [2] Maurette et al. (2000) Planet. Spac. Sci. 48, 1117. [3] Duprat J., et al. (2010) Science 328, 742-745. [4] Floss et al. (2009) LPSC XL, #1082. [5] Charon et al. (2017) LPSC XLVIII, #2085. [6] Zega et al. (2007) MAPS 42, 1373. [7] Floss C. et al. (2009) LPSC XL, #1082. [8] Haenecour et al. (2014) 11th International GeoRaman Conference, #5017. [9] Hily-Blant et al. (2013) Icarus 223, 582. [10] Floss et al. (2006) GCA 70, 2371. [11] Floss et al. (2012) LPSC XLIII, #1217. [12] Wiesman et al. (2014) LPSC XLV, #1509. [13] McSween & Huss (2010) Cambridge University Press. [14] Davidson et al. (2012) MAPS 47, 1748.

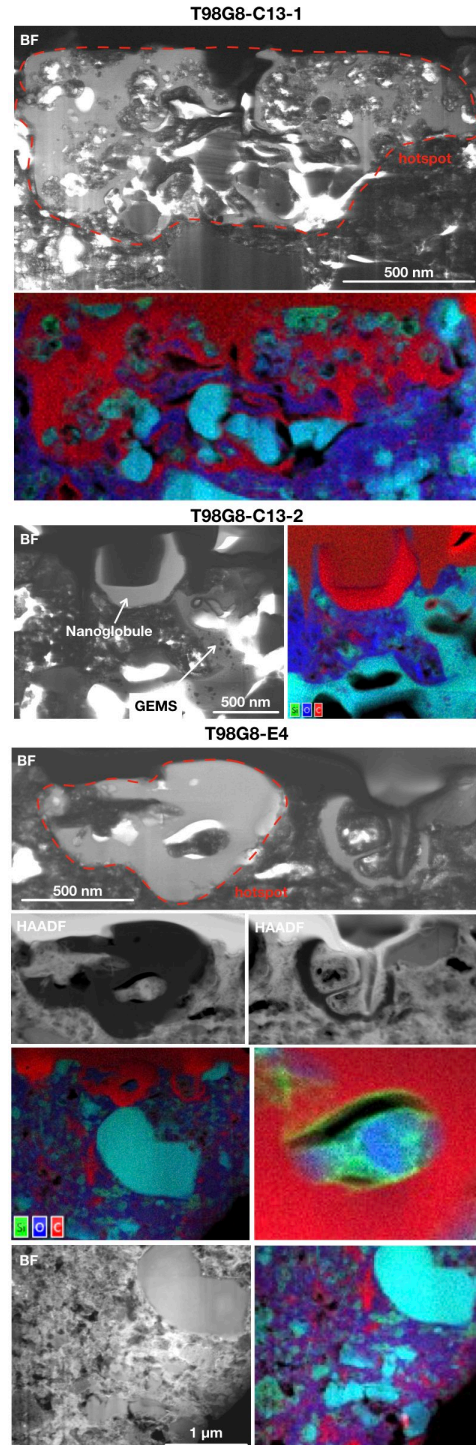


Fig. 2: Bright-field (BF), dark-field (HAADF) and EDS elemental maps (Si, O, C) of hotspots T98G8-C13-1, T98G8-C13-2 and T98G8-E4.

Acknowledgments. This work is supported by NASA Grant NNX15AD94G for the NExSS “Earths in Other Solar Systems” (EOS) program. TEM and FIB analyses were carried out at the University of Arizona Kuiper Materials Imaging and Characterization Facility (NSF Grant 1531243 and NASA Grants NNX15AJ22G and NNX12AL47G).